

Generation of Low-Energy Excitations in Silicon

Xiao Liu, P. D. Vu, and R. O. Pohl*

Laboratory of Atomic and Solid State Physics, Cornell University, Ithaca, New York 14853-2501

F. Schiettekatte and S. Roorda

Département de Physique, Université de Montréal, CP 6128 Succursale Centre-Ville, Montréal QC H3C 3J7, Canada

(Received 29 June 1998)

In order to understand the low-energy vibrational excitations common to amorphous solids, we have studied their evolution in ion-implanted crystalline silicon by measuring internal friction and heat conduction. The spectral density of these low-energy excitations evolves with increasing dose exactly towards that observed in the amorphous phase. More importantly, this evolution is unrelated to that of the amorphicity. We conclude that the defects in the crystal should be used to model the excitations in the amorphous silicon, rather than the amorphous structure itself. [S0031-9007(98)07337-2]

PACS numbers: 63.50.+x, 44.10.+i, 61.80.-x, 62.40.+i

Low-energy localized vibrational excitations, now commonly referred to as tunneling states [1] and widely studied through low temperature thermal and elastic measurements, have become accepted as a common feature of amorphous solids [2]. It is generally believed that they are caused by tunneling of atoms or groups of atoms between nearly degenerate minima in a potential determined by the amorphous structure [3,4]. Similar excitations have been found in some highly disordered crystalline solids [5–8], although it has remained unclear how these excitations are related to those of amorphous solids. In this Letter, we report the evolution of tunneling states in crystalline silicon which was gradually disordered by ion implantation. The important new result is that we have found no difference in their approach to saturation at the level characteristic for the amorphous phase regardless of whether the host amorphizes or not. We conclude that the primary cause of these tunneling states must be a disorder common to both the disordered crystalline and the amorphous phases, which rules out the amorphous structure itself.

Ion implantation into crystalline silicon (*c*-Si) displaces numerous atoms from their lattice sites, resulting in individual defects in the host that are stable at room temperature, such as divacancies and di-interstitials [9]. At ion energies in the range of 200 keV, implantation at room temperature with small power density (<50 mW/cm²) by ²⁸Si⁺ leads to amorphization at doses $>4 \times 10^{14}$ cm⁻² [10], while amorphization by ¹¹B⁺ under the same conditions would require doses $>2 \times 10^{16}$ cm⁻² [11]. The damage caused by ion implantation into a substrate is usually confined to thin layers. In this work, both Si⁺ and B⁺ ions were used. The evolution of the tunneling states and also of a well-known crystalline defect were monitored starting from a very early stage of the implantation, in which only point defects were expected to exist, up to the saturation of the defects. With the exception of a few high-dose Si⁺ implanted samples in which the implanted

layers became amorphous, all of our samples remained crystalline with different concentrations of point defects and small defect clusters in the implanted layers. The peak concentration of B in the implanted layers never exceeded 0.1 at.%. Two techniques were employed to detect the tunneling states, and to compare them within the tunneling model [1]: (i) Relaxational scattering of phonons at ~ 5.5 kHz by tunneling states, probed by implanting the neck of double-paddle oscillators, and measuring the internal friction, as described previously [12], and (ii) resonant scattering of thermal phonons (10–100 GHz), probed through heat conduction measurements on thin Si bars ($6 \times 50 \times 0.3$ mm³) cleaved out of the same high purity $\langle 100 \rangle$ Si wafers used to make the double-paddle oscillators, ions implanted into one of the large polished faces, with heat flowing in the long direction. In this experiment, the thermal phonon mean-free path ℓ_{layer} within the implanted layers was derived using a Monte Carlo technique as has been described elsewhere [13]. For the internal friction measurements, implantation with a consecutive increase of Si⁺ and B⁺ doses was done at Cornell Nanofabrication Facility at room temperature with energies of 50, 120, and 180 keV to achieve uniform disorder in the implanted layers to a depth of 400 and 680 nm, respectively. For the heat conduction measurements, larger layer thicknesses were required to improve the sensitivity. By using multiple implantation energies up to 5 MeV (6 MeV) for Si⁺ (B⁺), at the accelerators of the University of Montreal, uniformly implanted layers of 3.4 μ m (6.85 μ m) thick were achieved. Si⁺ implantation was done at 77 K [14], while for B⁺ implantation, the sample was carefully kept at room temperature by air cooling to ensure a disordered crystalline structure.

Rutherford backscattering and channeling was used to determine the disorder in the samples (see Fig. 1). The curve called “random” shows the strong backscattering (no channeling) of a misaligned unimplanted Si crystal. In a fully amorphized layer [Si⁺ dose: 7×10^{15} cm⁻²

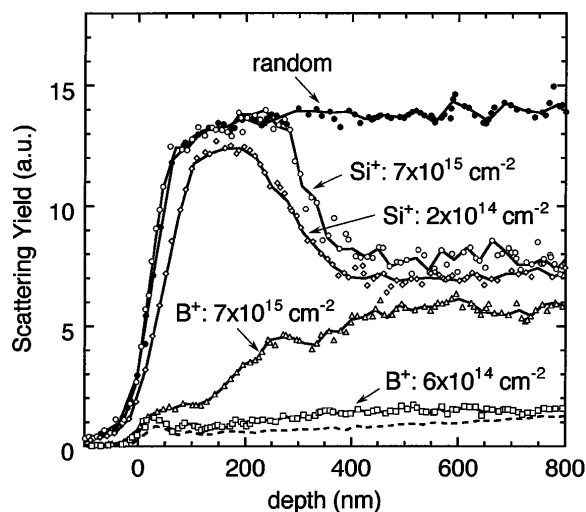


FIG. 1. Rutherford backscattering and channeling spectra, using 2.5 MeV He^{++} , of ion-implanted Si with implantation ion beam power density below 45 mW/cm². For two Si^+ implantations, doses at 50, 120, and 180 keV were $7 \times 10^{15} \text{ cm}^{-2}$ and $2 \times 10^{14} \text{ cm}^{-2}$. For two B^+ implantations, the energies and doses were the following: 50 keV, 7×10^{15} (6×10^{14}) cm^{-2} ; 120 keV, 7×10^{15} (9×10^{14}) cm^{-2} ; 180 keV, 7×10^{15} (1.32×10^{15}) cm^{-2} . The curve labeled “random” was obtained on a misaligned *c*-Si, while the dashed curve at the bottom is the aligned spectrum from unimplanted *c*-Si.

(see also the TEM picture in Ref. [12]), the same strong backscattering occurs throughout the amorphized layer (330 nm [12]), indicative of complete structural disorder. Note that even at a much smaller dose, $2 \times 10^{14} \text{ cm}^{-2}$, the backscattering is very large, evidence for the approach to amorphicity, in agreement with early studies [10]. In contrast, B^+ implantation of comparable doses leads to much less backscattering, indicative of a largely preserved crystal structure [11]. For the high dose, $7 \times 10^{15} \text{ cm}^{-2}$, we estimate that more than 85% of the Si atoms occupy crystalline lattice positions in the implanted layer, while for the smaller dose, $6 \times 10^{14} \text{ cm}^{-2}$, more than 95% of the Si atoms retain the long-range monocrystalline order [15].

In spite of this evidently different structural disorder, the internal friction of two samples implanted with Si^+ and B^+ with comparable doses, 3.5×10^{14} and $6 \times 10^{14} \text{ cm}^{-2}$ (for the smallest energy), respectively, is very similar (see Fig. 2). The dominating peak at 48 K is caused by a Debye relaxation associated with divacancies, which is believed to have an electronic origin. It has been identified as occurring in disordered *c*-Si, and becoming deactivated when the structure gets amorphized [12]. The important feature for the present investigation is the nearly temperature independent internal friction plateau observed for both samples. From the known implanted layer thicknesses and shear moduli [14,16] the temperature independent internal friction of the layers themselves, Q_{layer}^{-1} , can be calculated [17], $Q_{\text{layer}}^{-1} \approx 3.3 \times$

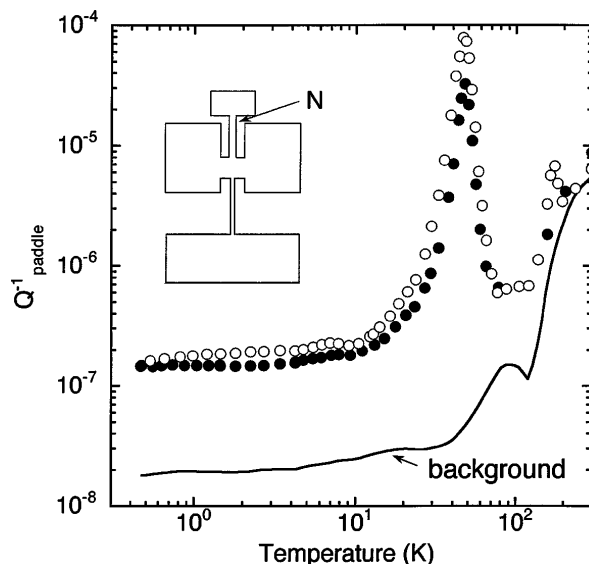


FIG. 2. Internal friction of an unimplanted paddle (background) and of two paddles ion-implanted on one side as described in the caption of Fig. 1. Solid circles: Si^+ doses of $3.5 \times 10^{14} \text{ cm}^{-2}$ for each of the three energies; open circles: B^+ doses of 6×10^{14} , 9×10^{14} , and $1.32 \times 10^{15} \text{ cm}^{-2}$ for 50, 120, and 180 keV, respectively. Inset: The schematic of the paddle oscillator. The neck (*N*) is implanted. In the vibrational mode studied, the neck is twisted around its long axis.

10^{-5} for either, which is smaller by a factor of 4 and 2 than that of amorphous silicon *a*-Si prepared by *e*-beam evaporation and sputtering, respectively [18]. A temperature independent internal friction plateau Q_0^{-1} of this order of magnitude is characteristic for amorphous solids, and is connected by the tunneling model [1] to the uniform spectral density \bar{P} of the tunneling states, their coupling energy γ to the phonons, the mass density ρ , and speed of sound v by

$$Q_0^{-1} = \frac{\pi}{2} \left[\frac{\bar{P}\gamma^2}{\rho v^2} \right]. \quad (1)$$

The term in square brackets is called the tunneling strength C . Its similar magnitude in almost all amorphous solids represents a major challenge to an understanding of the tunneling states on a microscopic level (see Refs. [17,18] for an exception found recently). It is known that *a*-Si prepared by ion implantation can be regarded as an essentially ideal random network with a few percent defects [19]. The similar magnitude of Q_{layer}^{-1} for both implanted layers suggests that this defect concentration may be more important in determining the internal friction than the total amount of disorder.

Next, we study the evolution of the low-energy excitations with increasing dose. For doses varying over 5 orders of magnitude, qualitatively similar internal frictions are observed, i.e., a divacancy peak and a nearly temperature independent plateau. Figure 3a shows the plateau value Q_{layer}^{-1} of the implanted layers measured at 3.4 K

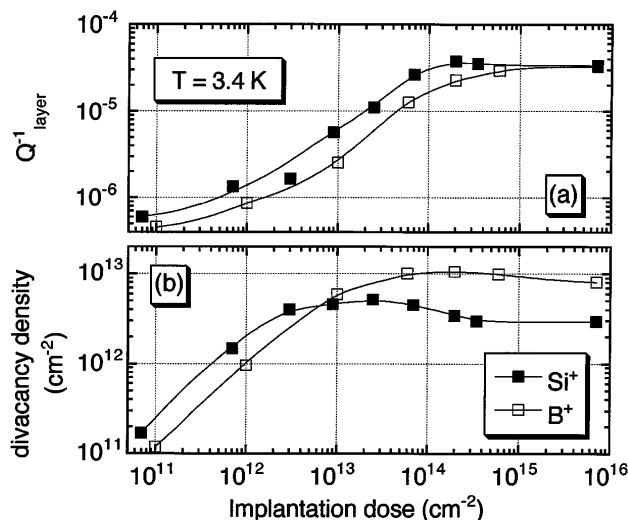


FIG. 3. (a) Q_{layer}^{-1} at 3.4 K as a function of implantation dose for the smallest energy, 50 keV. For B^+ implantation, the doses differed for the three energies as 1:1.5:2.2 for 50, 120, and 180 keV, except for the sample with the highest dose (see caption of Fig. 1). For the Si^+ implantation, the doses were the same at all three energies. (b) Divacancy density per implanted area. Note that for high Si doses, when the top 330 nm are amorphous, the excitations associated with divacancies are largely suppressed in the amorphous region, and occur mainly in the damaged crystalline layer underneath, about 70 nm thick [12].

as a function of implantation dose, while Fig. 3b shows the divacancy density determined from the peak at 48 K [12]. For both Si^+ and B^+ implantation, Q_{layer}^{-1} as well as divacancy defects form already at small doses. Q_{layer}^{-1} approaches its saturation value, 3.3×10^{-5} , for doses exceeding 10^{14} cm^{-2} , when even the Si^+ implanted layer is only partly amorphized, and the B^+ implanted layer shows only minimal disorder (see Fig. 1).

Before discussing details of the dose dependence, we want to test whether the states whose relaxation leads to the internal friction plateau have indeed the wide spectral density of states which is characteristic for amorphous solids [1]. According to the tunneling model, the same tunneling strength C also determines the thermal conductivity below ~ 1 K, although the resonantly scattered phonons sample a different part of the tunneling state spectrum [20]. This close connection between the internal friction plateau and the thermal conductivity has been tested successfully in many cases for bulk amorphous solids [2] as well as for disordered crystals [6], and constitutes a major success of the model [1]. Figure 4 shows the same test for Si^+ and B^+ implantation. The solid line is the predicted mean-free path ℓ_{layer} for thermal phonons traveling in the implanted layers based on the value of the measured Q_{layer}^{-1} when the saturation has been reached (shown in Fig. 3a), and the data points were determined from the heat conduction measurements for Si^+ and B^+ implanted samples with doses within the range of satura-

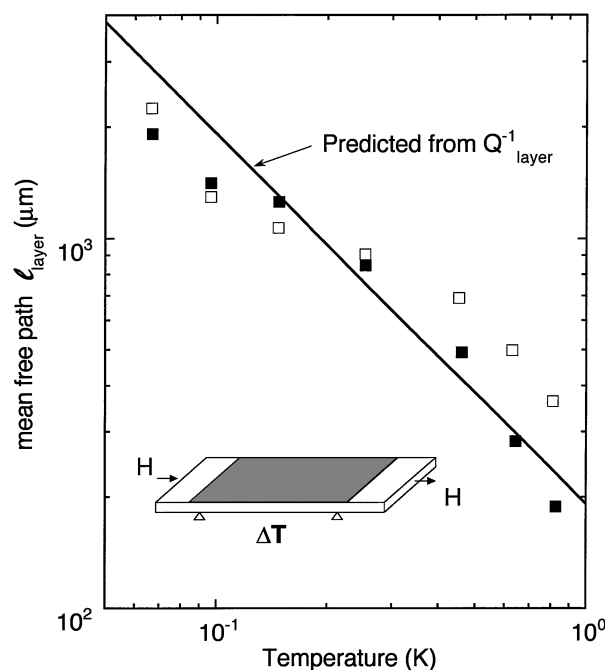


FIG. 4. Thermal phonon mean-free path ℓ_{layer} in layers which had been uniformly implanted by using multiple ion beam energies. Solid square: Si^+ , $3.4 \mu\text{m}$ thick amorphized layer, to an average concentration corresponding to 10^{15} cm^{-2} with a single energy at 50 keV; open square: $^{11}B^+$, $6.85 \mu\text{m}$, disordered crystalline, 10^{15} cm^{-2} ; solid line: phonon mean-free path as predicted from the plateau value of the internal friction $Q_{\text{layer}}^{-1} = 3.3 \times 10^{-5}$ of the layers as shown in Fig. 3a, using the tunneling model. Inset: Schematic of the heat conduction. Heat (H) is flowing along the length of the sample. The phonon scattering in the implanted layer (shaded area) leads to a temperature drop of ΔT .

tion (10^{15} cm^{-2} for both). The agreement shows that the excitations in both Si^+ and B^+ implanted layers have the broad, uniform spectral density that is characteristic for amorphous solids.

We now discuss the dose dependence. The divacancy density (see Fig. 3b) first increases linearly at low doses (approximately two divacancies per incident Si^+ and one for B^+), as is expected for the creation of isolated point defects [21]. Interaction between the divacancies, or some other perturbation of the crystalline environment, leads to a saturation of the divacancy peak at higher doses. The dropoff for even higher Si^+ doses is evidence for the deactivation of the divacancy peak in the amorphous phase. This dropoff is nearly absent for the B^+ implantation, which is taken as further evidence that B^+ implantation does not amorphize the host. Q_{layer}^{-1} , on the other hand, rises sublinearly at low doses (see Fig. 3a) and the slope of this rise increases steeply when the increase of the divacancy density slows down, until it finally saturates. Thus the formation of the tunneling states appears to depend on some interaction or random strains even at small doses. The formation accelerates as the strains build up,

until saturation is reached. This evolution is, however, *independent* of the amorphization, as shown by the fact that for a Si^+ dose of $6 \times 10^{13} \text{ cm}^{-2}$, when only a small fraction of the host is amorphized, Q_{layer}^{-1} is practically at its saturated level. Complete amorphization, which occurs at a 10 times larger Si^+ dose, does not lead to a further increase of the low-energy excitations. Moreover, exactly the same saturated Q_{layer}^{-1} is reached for B^+ implantation without ever amorphizing the host lattice at all.

In summary, our experiments show that implantation into the crystal leads to a gradual buildup of the tunneling states which are characteristic for amorphous solids. Yet, the amorphous structure is not their primary cause. This observation supports the recent discovery of the first amorphous solid, hydrogenated silicon, which has no low-energy excitations at all [17]. Instead, we suggest that these states may be understood in terms of individual defects in a random strain field. They persist, at their saturated level, in the amorphous phase, although they can equally exist in the crystal. Watson [22] has shown how random strains in crystals can lead to a broad distribution of tunneling states. Conceivably, in our experiments the strains will grow with dose until locally the yield stress is exceeded, leading to saturation. While our observations are restricted to silicon at this time, our conclusions may also be applicable to amorphous solids as well as to disordered crystalline solids with glasslike excitations [5–8]. As a previously ignored example for the latter, we suggest undoped alkali halide crystals, in which after exposure to ionizing radiation a low temperature thermal conductivity varying as T^2 has long been an unresolved puzzle [23]. This may have been an early observation of what we now call the evolution of glasslike excitations.

We thank Dr. R. S. Crandall of the National Renewable Energy Laboratory for numerous illuminating discussions. We also thank Dr. P. Revesz of the Ion Beam Laboratory of the Cornell Center for Material Research for his help with the RBS and channeling work, and Dr. P. Wagner of Wacker Siltronic, Burghausen, Germany, for supplying us with the ultrapure silicon wafers essential for this work. This work was supported by the Semiconductor Research Corporation under Grant No. 95/Sc/069, the National Science Foundation, Grant No. DMR-9701972, and the NREL FIRST Program. Additional support was received from the Cornell Nanofabrication Facility, NSF Grant No. ECS-9319005.

*Electronic address: pohl@msc.cornell.edu

- [1] W. A. Phillips, Rep. Prog. Phys. **50**, 1657 (1987).
- [2] P. A. Medwick, B. E. White, Jr., and R. O. Pohl, J. Alloys Compd. **270**, 1 (1998).
- [3] A. Heuer, Phys. Rev. Lett. **78**, 4051 (1997).
- [4] R. Kühn and U. Horstmann, Phys. Rev. Lett. **78**, 4067 (1997).
- [5] A. C. Anderson, Phase Transit. **5**, 301 (1985).
- [6] K. A. Topp and D. G. Cahill, Z. Phys. B **101**, 235 (1996).
- [7] A. Vanelstrate and C. Laermans, Phys. Rev. B **42**, 5842 (1990).
- [8] M. A. Ramos, S. Vieira, F. J. Bermejo, J. Dawidowski, H. E. Fischer, H. Schober, M. A. González, C. K. Loong, and D. L. Price, Phys. Rev. Lett. **78**, 82 (1997).
- [9] R. J. Schreutelkamp, J. S. Custer, J. R. Liefting, W. X. Lu, and F. W. Saris, Mater. Sci. Rep. **6**, 275 (1991).
- [10] G. Bai and M. A. Nicolet, J. Appl. Phys. **70**, 649 (1991); **70**, 3551 (1991).
- [11] J. E. Westmoreland, J. W. Mayer, F. H. Eisen, and B. Welch, Appl. Phys. Lett. **15**, 308 (1969); E. C. Baranova, V. M. Gusev, Yu. V. Martynenko, C. V. Starinin, and I. B. Haibullin, Radiat. Eff. **18**, 21 (1973); Y. Akasaka, K. Horie, K. Yoneda, T. Sakurai, H. Nishi, S. Kowabe, and A. Tohi, J. Appl. Phys. **44**, 220 (1973).
- [12] Xiao Liu, R. O. Pohl, R. S. Crandall, and K. M. Jones, Mater. Res. Soc. Symp. Proc. **469**, 419 (1997).
- [13] P. D. Vu, J. R. Olson, and R. O. Pohl, J. Low Temp. Phys. (to be published).
- [14] D. L. Williamson, S. Roorda, M. Chicoine, R. Tabti, P. A. Stolk, S. Acco, and F. W. Saris, Appl. Phys. Lett. **67**, 226 (1995).
- [15] W. K. Chu, J. W. Mayer, and M. A. Nicolet, in *Backscattering Spectrometry* (Academic Press, New York, 1978), pp. 255–263.
- [16] R. Vacher, H. Sussner, and M. Schmidt, Solid State Commun. **34**, 279 (1980).
- [17] Xiao Liu, B. E. White, Jr., R. O. Pohl, E. Iwanizcko, K. M. Jones, A. H. Mahan, B. N. Nelson, R. S. Crandall, and S. Veprek, Phys. Rev. Lett. **78**, 4418 (1997).
- [18] Xiao Liu and R. O. Pohl, Phys. Rev. B (to be published).
- [19] S. Roorda, W. C. Sinke, J. M. Poate, D. C. Jacobson, D. Dierker, B. S. Dennis, D. J. Eaglesham, F. Spaepen, and P. Fuoss, Phys. Rev. B **44**, 3702 (1991).
- [20] Properly averaged over the transverse and longitudinal deformations (see, e.g., Ref. [6]).
- [21] B. S. Berry and W. C. Pritchett, in *Ion Implantation in Semiconductor 1976*, edited by F. Chernow, J. A. Bordes, and D. K. Brice (Plenum, New York, 1977), p. 435.
- [22] S. K. Watson, Phys. Rev. Lett. **75**, 1965 (1995).
- [23] C. T. Walker, Phys. Rev. **132**, 1963 (1963).